Real-time Compensation of Dynamic Thermally Induced Optical Aberrations by a Deformable Mirror Based on Reluctance Actuators

R.F.M.M. Hamelinck[1], P.R. Fraanje[1,2], N.J. Doelman[1]
[1] *TNO Science and Industry, the Netherlands*
[2] *Delft University of Technology, the Netherlands*

r.hamelinck@tno.nl

1 Introduction

The resolving power of an optical system is often limited by the presence of time-varying wavefront distortions caused by heat flows. The aberrations do not only include tip/tilt and focus terms, but also higher spatial frequencies, due to the heat flow's turbulent nature. TNO has built an adaptive optics (AO) breadboard, to demonstrate the correction of thermally induced wavefront aberrations using various control algorithms and a deformable mirror (DM) based on reluctance actuators [1].

2 The adaptive optics breadboard

Figure 1 shows the AO breadboard with the optical rays drawn for clarification.

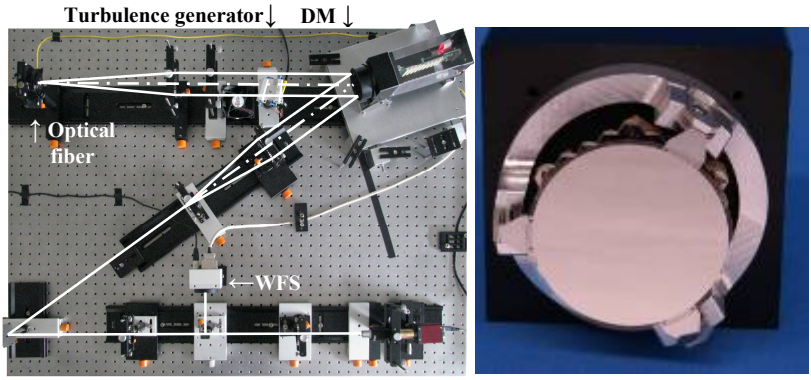

Figure 1: Photo of the AO breadboard at TNO (left). Photo of the DM with 61 reluctance actuators, as used on the AO breadboard (right).

An optical fiber delivers a point source. After collimation the light reflects on the DM. An electrical resistor and fan act as a turbulence generator and are placed below the collimated beam, approximately 20cm in front of the DM. After reflection the beam size is decreased and split for the Shack Hartmann lenslet array with wavefront sensor camera (Imperx IPX-VGA210L) and for the science camera. The latter re-images the point source. Control is done with a general purpose PC with real-time Linux operation system. The sampling rate is equal to the frame rate of the wavefront sensor camera and is given by 140Hz.

2.1 The deformable mirror

The breadboard is built to demonstrate different control algorithms and to test the recently developed deformable mirror based on reluctance actuators [1]. That mirror consists of a thin continuous facesheet on which the push-pull actuators impose the out-of-plane displacements. The 61 variable reluctance actuators, located in a modular actuator grid have ±10μm stroke with nanometer resolution. The facesheet is chosen thin for its low moving mass and out-of-plane stiffness, thereby preventing large power dissipation and the need of active cooling. Each actuator consists of a closed magnetic circuit in which a permanent magnet provides static magnetic force on a ferromagnetic core in a membrane suspension. This force is influenced by a current through the coil which is situated around the magnet to provide movement of the core. Figure 2 shows a Zernike table generated with the DM and measured by an interferometer.

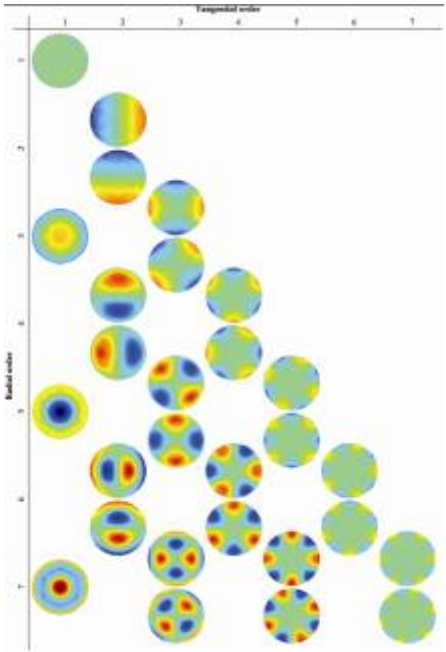

Figure 2: Zernike table generated by the DM and interferometrically measured.

2.2 Control

The controller in the AO system has a disturbance rejection task; the turbulence-induced wavefront distortions need to be reduced by actuation of the DM. A commonly used approach in AO systems is to minimize the variance of the wavefront error. The input to the control system is provided by a Shack-Hartmann type wavefront sensor, which measures spatial gradients of the wavefront in horizontal and vertical direction at 76 points evenly distributed over the aperture. This results in a 152 dimensional sensor signal from which the wavefront phases can be retrieved by spatial integration. The transfer between the actuator controls and the wavefront sensor signals can be approximated with a static matrix, the poke matrix, and two samples delay (1 sample delay from the exposure time of the camera and 1 sample delay from the digital controller). The controller consists of an integrator in series with a matrix that inverts the poke matrix. In fact a pseudo inverse is used which only inverts the 30 dominant singular values while setting the other singular values to zero.

3 Experimental results

Figure 3 shows a snapshot of the observed turbulence in open and in closed loop. Figure 4 shows the spatially averaged power spectral densities of the reconstructed wavefront phase in open and closed loop. The bandwidth is about 7Hz, which is a factor 10 smaller than the Nyquist frequency. Figure 5 shows the energy per

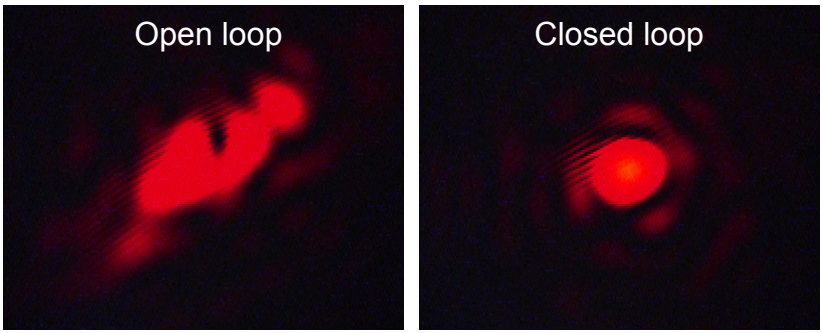

Figure 3: Snapshots of the science camera view in open and closed loop.

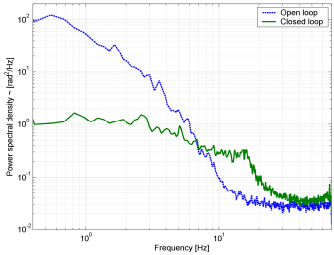

Figure 4: Spatially averaged PSD in open and closed loop.

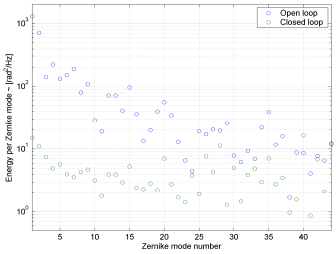

Figure 5: Energy in various Zernike modes in open and closed loop.

Zernike mode [2], where the modes are numbered from 1 to 44, in the order Z_1^{-1}, Z_1^{1}, Z_2^{-2}, Z_1^{0}, Z_2^{-2}, ..., Z_8^{8}. From Figure 5 is observed that the Zernike mode Z_1^{-1} is suppressed with a factor 86 and all Zernike modes are reduced approximately to the same level. From Figure 4 it is observed that the slope of the open loop average PSD is between -20dB/dec and -40dB/dec, which is common for turbulent disturbances. As a consequence the optimal one-step ahead predictor is different from a pure integrator, and thus further performance improvement can be obtained by using an (optimal) predictor rather than an integrator as was demonstrated in [3]. Comparison with the method in [3] as well as adaptive predictors will be future work.

4 Conclusions

Thermally induced aberrations have been effectively compensated by control of a deformable mirror with 61 reluctance actuators using integral feedback. Further work will include prediction methods to improve the disturbance attenuation.

References:

[1] R. Hamelinck, R. Ellenbroek, N. Rosielle, M. Steinbuch, M. Verhaegen and N. Doelman. Validation of a new adaptive deformable mirror concept. In N. Hubin, C.E. Max and P.L. Wizinowich, editors, *Proceedings of SPIE: Astronomical telescopes and instrumentation*, volume 7015, Marseille, France, June 2008.

[2] M. Born and E. Wolf, Principles of Optics, Oxford, Pergamon, 1970.

[3] K. Hinnen, M. Verhaegen and N. Doelman, "*A Data-Driven H2-Optimal Control Approach for Adaptive Optics*", IEEE Transactions on Control Systems Technology, Vol. 16, No. 3, pp. 381- 395.